eprints@whiterose.ac.uk
https://eprints.whiterose.ac.uk/

Materials Optimization for Magnetic MEMS

Mike R. J. Gibbs

Sheffield Centre for Advanced Magnetic Materials & Devices (SCAMMD), Department of Engineering Materials, University of Sheffield, Sheffield S1 3JD, U.K.

By highlighting magnetomechanical effects such as the ΔE-effect, and developing modeling code that integrates magnetoelasticity with microelectromechanical systems, it is shown that a simple cantilever system can have a sensitivity to mass loading at the attogram level. The requirements on the magnetoelastic materials for such devices are described, and progress towards achieving optimized material is reviewed. The possibility for deployment of such systems in security, healthcare, and bioscience is outlined.

Index Terms—**Magnetic layered films, magnetostrictive devices, microelectromechanical devices.**

I. INTRODUCTION

THERE are a number of examples in the literature where magnetic materials have been incorporated in to microelectromechanical systems (MEMS) [1], [2]. From hereon we will use the diminutive MagMEMS when referring to MEMS incorporating magnetic material [3].

The integration of magnetic components in to MEMS, MagMEMS, offers several key advantages over other MEMS technologies. Primary amongst these is the ability to develop wireless technology. In comparison to other MEMS technologies, especially those incorporating piezoelectric materials, MagMEMS offer a higher power density, low performance degradation, fast response times, ease of fabrication and self test/self calibration functions [1], [3], [4]. A magnetic element may be interrogated by inductive coupling; the permeability or the resonant frequency of a structure containing the element being a function of stress, strain, pressure or other measurands due to the magnetoelastic properties of the magnetic material. The current macroscopic anti-theft sensors in stores rely on such a principle. This capability immediately opens up the possibility of applications in remote or hostile environments, and provides a mechanism for self-test and self-calibration [3]. Magnetic films have been successfully deposited on a wide range of substrates; conventional materials such as Si or GaAs, and also polymers (Kapton) and glass. MagMEMS structures should not be assumed to require standard Si microfabrication, as other materials such as glasses or polyamides can be patterned using lithography or printing.

A range of proof-of-concept, or proof-of-principle, sensors and actuators based on MagMEMS have been demonstrated in recent years [1]–[6]. In particular the use of thin film magnetoelastic materials in MagMEMS has been considered [7], [8], but only in terms of measurement of saturation magnetostriction constant, and related properties such as the ΔE-effect. Optimization of these properties for device applications, including the holistic aspects of the system performance, has not been addressed.

For the purposes of this discussion we will consider a cantilever beam as the MEMS platform, to which we shall add func-
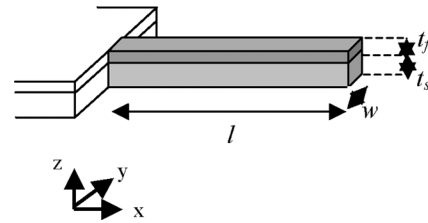

Fig. 1. Schematic illustration of the basic cantilever structure. The cantilever length is l, width w and thickness is t_s. The magnetic film and active layer coating the beam has thickness t_f and the same lateral dimensions as the MEMS cantilever.

tionality by the introduction of magnetic material. A simple embodiment is sketched in Fig. 1.

In all that follows the MEMS platform will be assumed to be a typical tipless atomic force microscopy (AFM) cantilever currently in mass production. The reason behind this is that, in this exercise, we are highlighting the functionality achieved by the magnetic material, and wish to place no unusual constraints on the MEMS platform towards this goal.

Joule magnetostriction, the change in dimensions of a ferromagnet on the application of an applied magnetic field, offers actuation in this context. If a magnetic field is applied in the +x direction in Fig. 1 then, for a material having a positive saturation magnetostriction, there will be a length increase along +x. In such a bimorph structure this will lead to deflection of the cantilever in −z, and contraction in ±y. This gives mechanical actuation. Conversely, the mechanical deflection of the tip of the cantilever in ±z, will lead to a change in permeability of the magnetic film by the Villari effect (the inverse of the Joule effect). Thus a sensing function is possible.

There have been attempts at an analytical model of the bending of a MEMS cantilever beam under the influence of a coating layer of magnetostrictive material. Earlier work in this group using an adaptation of a finite element technique, demonstrated that these models were limiting cases of a more general response of such a system [9]. This has recently been more firmly established in this group using a finite element package (COMSOL), based on a multi-physics approach, that has allowed direct coupling of the magnetostriction tensor with the structural mechanics of a MEMS cantilever [10]. Agreement within a few percent was achieved with the various available analytical models, and important bending and curling modes have been demonstrated, as a function of width to length ratio

of the cantilever, not apparent from any earlier models. Also by modal analysis, it has been possible to establish physical attributes for the cantilever structure which will be necessary for mono-mode excitation, important for systems. At this stage ideal performance of the magnetic material has been assumed; that is magnetization by pure moment rotation of a single domain state. Further details are given in Section III. Future work, including the integration of micromagnetic modeling with MEMS models will be needed for more detailed analysis. Work on this is ongoing in the group, and will be reported elsewhere.

There is a very important magnetic characteristic missing from all of the previous modeling, the ΔE-effect, the field dependence of the Young's modulus in highly magnetostrictive materials. We will discuss this in the context of a MagMEMS sensor.

In order to consider the significance of the ΔE-effect, we first investigate the deflection of a simple cantilever coated with magnetostrictive material. It has been shown [9] that a satisfactory empirical formula for the free end deflection, δ, of a cantilever of length l and width w, and for a magnetic film of thickness t_f and a substrate of thickness t_{sub} comprising the cantilever, is given by

$$\delta = \frac{9}{2} \frac{l^2 t_f}{t_{\text{sub}}^2} \lambda_s \frac{E_f}{E_{\text{sub}}} \frac{\left(1 + \left(\frac{l}{l+w}\right)\nu_{\text{sub}}\right)}{(1+\nu_f)} \quad (1)$$

where $E_{\text{f,sub}}$ and $\nu_{\text{f,sub}}$ are the Young's modulus and Poisson's ratio of film and substrate, respectively. λ_s is the saturation magnetostriction constant. Taking the following typical parameters for an AFM cantilever with a magnetostrictive film coating, $l = 40$ mm, $w = 1$ mm, $t_{\text{sub}} = 400$ μm, $t_f = 100$ nm, $E_{\text{sub}} = 70$ GPa, $E_f = 220$ GPa, $\nu_{\text{sub}} = \nu_f = 0.25$ and $\lambda_s = 20 \times 10^{-6}$ yields $\delta = 280$ nm. Deflections of this order have been observed [11].

Because the magnetization is coupled to an applied strain via magnetostriction, there is more strain for a given load in an applied field than in zero applied fields. The total strain on the application of a load, ε, is made up of an elastic, ε_{el}, and a magnetostrictive, ε_λ, part, whence [12]

$$\varepsilon = \frac{\sigma}{E_s} + \frac{3\lambda_s}{2}\left(\frac{\mu_0^2 M_s^2 H^2}{(2K - 3\lambda_s \sigma)^2} - \frac{1}{3}\right) \quad (2)$$

where M_{s} is the saturation magnetization and K the anisotropy constant. Here E_{s} is the Young's modulus in magnetic saturation.

If we define E_H as the Young's modulus after application of a field, then

$$\frac{E_s - E_H}{E_H} = \frac{\Delta E}{E_H} = \frac{9\lambda_s E_s \mu_0^3 M_s^2}{(2K - 3\lambda_s \sigma)^3}H^2 = \Im H^2 \quad (3)$$

and the Young's modulus is a function of magnetic field. Experimental data on bulk amorphous ferromagnetic ribbons demonstrating this effect are shown in Fig. 2. The effect reaches a maximum when the anisotropy field, H_a, is reached such that

$$\left.\frac{\Delta E}{E_S}\right|_{\text{max}} = \frac{9\lambda_s^2 \mu_0 E_s}{(2K - 3\lambda_s \sigma)} = \frac{9\lambda_s^2 \mu_0 E_s}{H_A M_s}. \quad (4)$$
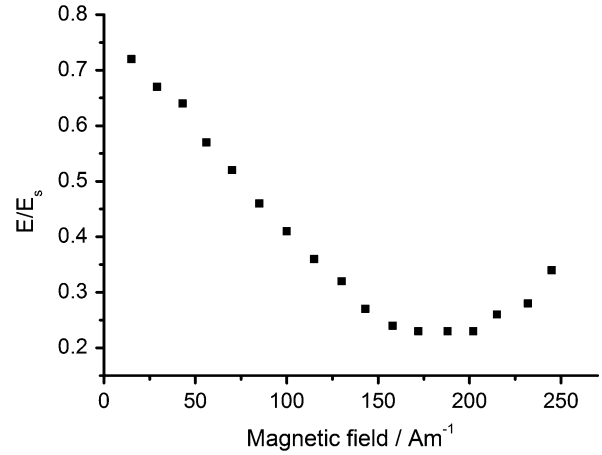

Fig. 2. Ratio of Young's modulus to saturation modulus versus applied field for METGLAS 2605SC ribbon field annealed to give close to pure 90° moment rotation on the application of the field. After [14].

We have previously demonstrated a proof-of-concept Mag-MEMS pressure sensor based on this phenomenon [13]. The resonant frequency of a SiN microbridge coated in magnetoelastic material was shown to be a function of magnetic field. The earlier work [13] had not optimized the performance, and so should be taken as illustrative only. The significance of a ΔE-effect will now be developed further.

The importance of this result for MagMEMS is best seen by investigating the systems aspects of the problem. We will consider here a sensor that works on the principle of an active layer (polymeric for the sake of this discussion) coated on to the surface of a MagMEMS cantilever adsorbing a chemical species over its sensing surface. For simplicity, it is assumed that this adsorption increases the mass loading on the sensor, and thus translates into a change in density of the sensing layer (it is further assumed that the thickness of adsorbate is much less than the thickness of the sensing layer).

If f_0 is the fundamental resonant frequency of the compound cantilever sketched in Fig. 1, then

$$f_0 = 0.162\sqrt{\frac{E}{\rho}}\frac{t^2}{l^2} \quad (5)$$

f_0, is dependent on the cantilever's thickness (t) and length (l) and on the properties of the material such as the Young's modulus E and the density ρ. For modeling purposes, ρ can be taken as the average density of the beam components where more than one layer is involved. (5) is for a very simple cantilever and pinned at one edge. We will later consider in more detail the sensitivity which may be achieved, but move on first to a discussion over the choice of magnetoelastic material that can be optimized for such applications.

This principle has been exploited by Grimes *et al.* [15], but the ultimate sensitivity of such a system is determined to first order by the overall dimensions, and hence MEMS processing is required. Also, this work did not optimize the magnetic material for the task.

II. MAGNETOELASTIC MATERIALS

A. Principles

The Joule magnetostriction, the Villari effect, and the ΔE-effect show the greatest response if the magnetization in the film rotates by 90° in the film plane [12]. In practical terms, this requires a material which can support a uniaxial anisotropy in a direction dictated by the sensor geometry. In order to maintain low power requirements in actuation the anisotropy field must also remain low, that is the anisotropy should be weak. We go on to consider the composition and preparation of films that can satisfy this criterion.

B. Composition Choices

In terms of low anisotropy field, high permeability and useful levels of saturation magnetostriction the amorphous ferromagnets based on around 80at% Fe are strong candidates. Around this composition λ_s the saturation magnetostriction constant is isotropic with a value of ~ 20 ppm. When first introduced as rapidly solidified ribbon, the Fe-based amorphous ferromagnets showed that simple thermal treatments could be used to control both the magnitude and direction of the magnetic anisotropy, and that the piezomagnetic response followed this [14], [16]. More recently these results have been replicated for thin films of Fe-based amorphous ferromagnets [17], [18]. Fig. 3 shows that standard lift-off processing can produce structures with good geometrical definition. 500 nm thick films of the same composition as METGLAS 2605SC (used as the target), grown on glass, can be produced with coercivities as low as 20 A/m and anisotropy fields as low as 100 A/m after a simple post-deposition annealing treatment [18]. A thermal treatment at 400 °C for 60 min in a vacuum of 10^{-2} Torr is sufficient to relieve stress remaining from the deposition process. The films are also capable of responding to annealing in the presence of a magnetic field, a well established technique for the METGLAS alloys in ribbon form [16]. A field of 0.3 T applied in the film plane, for the same temperature and time as the stress relief anneal, gave a weak uniaxial anisotropy in the forming field direction [18]. Fig. 4 shows the domain pattern and hysteresis loop for a sample that has been field annealed after deposition.

Taking published data [19] for METGLAS 2605SC ($E_s = 100$ GPa, $\lambda_s = 32$ ppm), and the experimentally determined anisotropy field after field annealing, an estimate of $\Delta E/E_s|_{\min} = 0.35$ is obtained by use of (4).

Using an $Fe_{70}B_{20}Si_6C_4$ target, Chiriac *et al.* [8] prepared amorphous ferromagnetic films on a polysilicon substrate, and determined basic magnetoelastic properties such as the saturation magnetostriction constant. From their tabulated data $\Delta E/E_s|_{\min} = 0.35$ was also determined from (4).

In terms of increasing values of λ_s the next set of alloys to consider are based on polycrystalline Fe-Co. The alloy series has been studied in bulk form for many years [20] with a bcc solid solution existing across the composition range of 0%–60% Co. The saturation magnetostriction constant λ_{100} peaks at the disordered equi-atomic composition, with a value of 150 ppm. Taking published data for the saturation magnetostriction constants of $Fe_{50}Co_{50}$ [20], [21], an isotropic

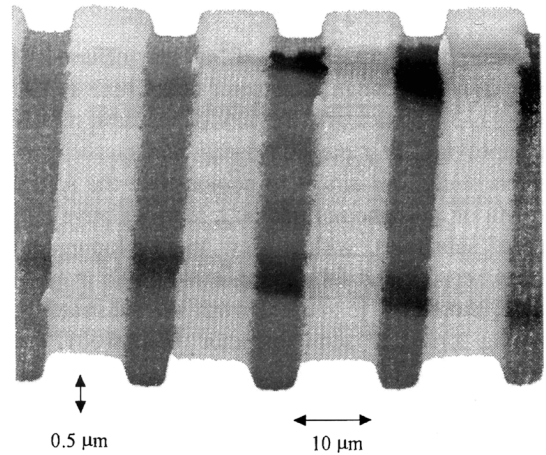Fig. 3. An AFM image of etched amorphous FeSiBC wires with nominal separation 5 μm, wire width 10 μm and thickness 0.3 μm on a Corning 7059 glass substrate (after [17]).
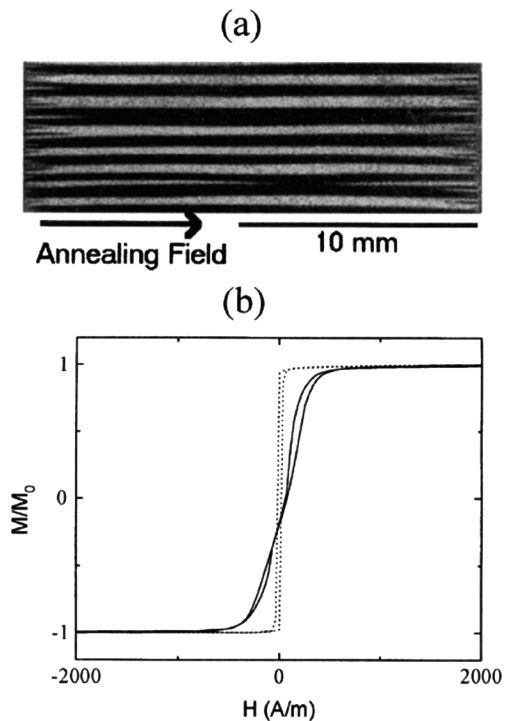

Fig. 4. (a) Domain image of a field-annealed amorphous ferromagnetic film. (b) magneto-optic Kerr effect hysteresis loops (in two orthogonal directions) taken from the central region of image (a). The asymmetry is an instrumental artifact (after [18]).

polycrystal should show a net magnetostriction constant of approximately 80 ppm. We have demonstrated [22] that this level of magnetostriction can be achieved in polycrystalline 300 nm thick films on glass substrates, but at the expense of coercivities greater than 500 A/m even after annealing. The anisotropy field was 3800 A/m. Using (4), and other published data [21] this also predicts $\Delta E/E_s|_{\min} = 0.35$. This is similar to that in the amorphous ferromagnets, but requires a much greater magnetic field. It must be pointed out that both anisotropy field and coercive field are functions of film thickness, grain size, and residual strain in the films. Work continues to explore routes to produce highly textured FeCo films, using appropriate seed
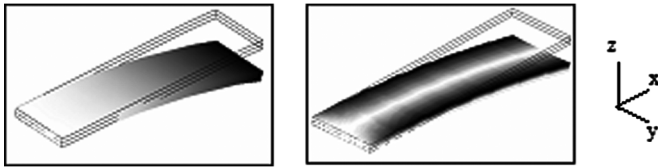
Fig. 5. Output from COMSOL simulation of the beam deflection (after [10]). (a) the deflection in z, (b) the deflection in y, showing the edge curling effects that can occur for $w/l > 0.1$, where w is the cantilever width and l the length. (Black highlights a greater deflection along the axis measured.)

layers, in order to achieve higher net magnetostriction constants for the films.

Whilst still in a more developmental stage, the Fe-Ga-Al alloys (Galfenol) offer even higher λ_s of more than 200 ppm [23]. Thin films are being studied [24], and with more characterization and studies of alloying additions may offer an additional alloy series for MagMEMS.

Traditionally high λ_s of more than 500 ppm has come from alloys containing RE elements, the archetype being the Tb-Dy-Fe series (Terfenol). Honda *et al.* [25], [26] were one of the first to research fabricating a cantilever device using magnetostrictive materials. From rare earth films of Tb-Fe and Sm-Fe, they developed a bimorph actuator found to have a large deflection even within a low magnetic field, but still higher than the anisotropy fields of the amorphous ferromagnets discussed above. The RE-containing materials are better suited for actuation than sensing.

In general, there are several alloy series which already, or with some further development, offer significant promise for MagMEMS. Further work is required on the production of controlled domain structure (leading to magnetization by pure moment rotation), but the preliminary work, based on equivalent bulk alloy forms, shows considerable promise. In device applications it may not always be the highest magnetostriction that is required, but rather the highest differential response at a given bias field (including zero field) that is important. This will be exemplified below.

III. System Modeling

We have used COMSOL to model the simple cantilever system defined in Fig. 1, [10]. It is important to characterize the mechanical properties of the system, as this gives design criteria for a successful device. Assuming uniform rotation of the magnetization (Stoner-Wohlfarth behavior), and having coupled the full magnetostriction tensor to the MEMS module provided in the multi-physics package, the mechanical deflection of the cantilever (see Fig. 1) has been studied. Fig. 5 shows the modes of deflection that can be observed. Provided the width to length ratio of the cantilever, w/l, is less than 0.1 the cantilever is stiff in the y-direction.

It is also important to optimize the relative thickness of the layers in the overall cantilever structure, in order to ensure maximum sensitivity to magnetostrictive stimulus. Fig. 6 shows a comparison of the tip deflection with an analytical model for the maximum deflection of a cantilever [27]. The FEM and analytical models agree very well, with the FEM allowing a wider range of analysis. Fig. 6 also gives an indication of the overall
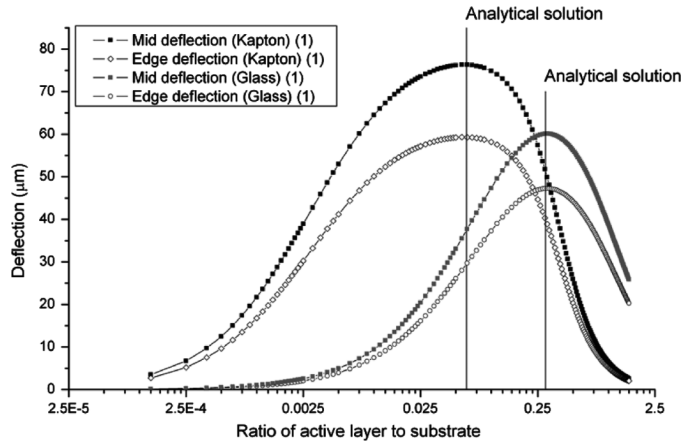

Fig. 6. Deflection of a cantilever made with a glass or Kapton base layer as a function of the relative thickness of the active (magnetostrictive) layer to the base layer. The vertical lines illustrate the analytical solutions of [26]. The width to length ratio has not been optimized to reduce curling in this instance.
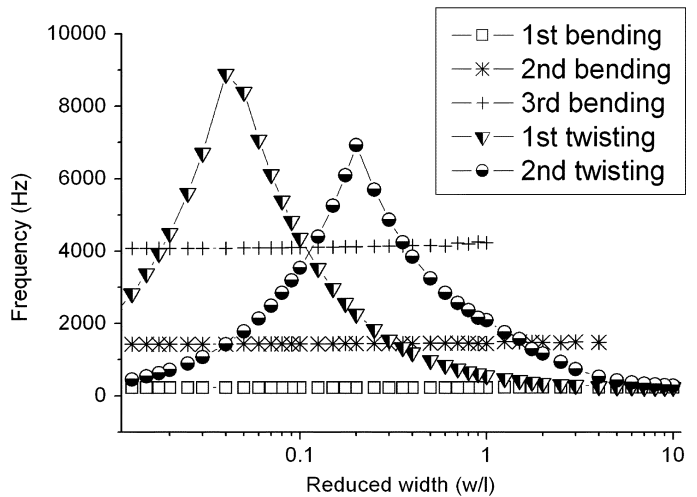

Fig. 7. Modal frequencies of a cantilever as a function of width to length ratio.

impact of the mechanical properties of the base material of the cantilever, by comparing data for glass and Kapton, a polyimide. A lower modulus base layer gives a greater deflection, but with more curling.

For a sensor system, the cantilever will be used under AC excitation. Either a rotating magnetic field can be applied, or more likely, a field pulse is used to excite the natural vibrational frequency (first bending mode) of the cantilever. Fig. 7 shows the modal response of the cantilever as a function of w/l. These data have also been generated in the COMSOL environment. For $w/l > 0.1$, the first bending mode is well separated in frequency from other modes, and there will be little cantilever curling.

IV. MagMEMS System

These data give us sufficient confidence in the advanced FEM model, to proceed to the modeling of a MagMEMS system.

To provide a context, and set a target for MagMEMS, we will consider the work of Ilic *et al.* [28] where a similar cantilever structure, but with a paddle shaped end, was used to detect added mass in a biological context. The sensing principle was optical

rather than piezomagnetic. This requires the ability to get an optical signal in and out of the sensor, and our goal is to demonstrate that with the wireless MagMEMS equivalent, a similar goal may be achievable. Ilic *et al.* [28] report attogram sensitivity, roughly equivalent to one strand of DNA added to the cantilever.

In order to highlight the practicalities of MagMEMS we will limit ourselves to MEMS cantilevers that are commercially available (tipless) for atomic force microscopy. Fabrication of such cantilevers is routine. For this model it is taken that a silicon wafer had a thermal oxide layer grown on its surface (SiO_2), and on top of this again was grown 30 nm of low stress SiN by chemical vapor deposition. The properties of this SiN layer, $E_s = 179$ GPa, $\rho = 2300$ kgm^{-3} and $\nu = 0.28$ are an average of values reported for this material. On top of this again was grown a 50 nm thick layer of METGLAS 2605SC by sputtering. This layer has properties $E_s = 100$ GPa, $\rho = 7300$ kgm^{-3} and $\nu = 0.3$ [19] assuming the film properties mimic the bulk form. We have already discussed in Section I how this structure can function as a sensor or actuator.

A standard bio-polymer, that may be functionalized to bind to a specific species (protein, toxin, antibody, etc.), has physical properties of $E_s = 2.8$ GPa, $\rho = 1100$ kgm^{-3} and $\nu = 0.3$ [29]. Such a film (say 100 nm thick) can be added to the magnetic layer in the cantilever structure. Standard release procedures can then produce free standing cantilevers which resemble the schematic in Fig. 1.

In order to determine the mass loading sensitivity, we have run the model by converting added mass adsorbed by the bio-polymer in to the equivalent density change. On the scale of mass adsorption in which we are interested, the system dimensions can be assumed constant. This density change is then fed in to the calculation of resonant frequency. It is further assumed, for simplicity of calculation, that the mass is adsorbed as a uniform layer over the cantilever surface. Fig. 8 is a plot of the shift in resonant frequency as a function of added mass, in steps of 1 attogram (equivalent to a 5 ng cm^{-2} added to the cantilever surface).

The validity of this highly linear response can be validated by further manipulation of (4) for the fundamental mode of the cantilever, f_r, where

$$f_r = 0.162 \sqrt{\frac{E}{\rho} \frac{t^2}{l^2}} = K\rho^{-\frac{1}{2}}. \tag{6}$$

If f_r' is the resonant frequency after mass loading, then

$$f_r' = K(\rho + \Delta\rho)^{-\frac{1}{2}} = K\rho^{-\frac{1}{2}} \left(1 + \frac{\Delta\rho}{\rho}\right)^{-\frac{1}{2}}. \tag{7}$$

For $\Delta\rho \ll \rho$

$$f_r' = K\rho^{-\frac{1}{2}} \left(1 - \frac{\Delta\rho}{\rho}\right) = f_r \left(1 - \frac{\Delta\rho}{\rho}\right). \tag{8}$$

For small added mass (change in density) the frequency shift is linear, and this is the response delivered from the model.

The gradient of the line in Fig. 8 gives a sensitivity of approximately 7.5 Hz/(ng cm^{-2}). The analytical model used here
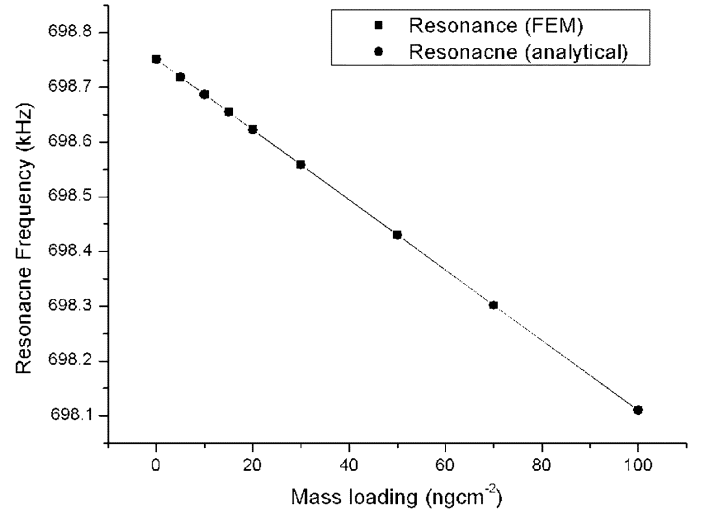

Fig. 8. Shift in resonance frequency of a cantilever as a function of added mass. The agreement between the models is to be noted.

is equation [8] with a volume average for the Young's modulus and density of the system. Again, there is excellent agreement between the analytical model and the simulation.

Such a small frequency shift would be difficult to detect in absolute terms. However, if we exploit the ΔE-effect set out above, and a high Q detector, then the resonant frequency will be a function of applied field through the field dependence of E. Adsorption of material changes the density and hence the resonant frequency. The measurement of the added mass comes from the DC field necessary to bring the sensor back on to resonance, which can be simply enabled. This makes for a very simple detection system.

The magnitude of the frequency shift at this level of sensitivity is such that we only need to shift the Young's modulus by mPa to return to resonance. The field sensitivity, the gradient in Fig. 2, is the most important feature, and it is this differential response which needs to be optimized.

We have chosen in this exercise to demonstrate that MagMEMS can offer the same level of sensitivity as more conventional MEMS, but hasten to point out that in many application areas this high level of sensitivity may be inappropriate.

V. THE NEXT STEPS

As indicated above, there is still much to be gained in the study of MagMEMS from the optimization of the magnetic layers in terms of anisotropy control. Greater flexibility in modeling, and the ability to quantitatively correlate modeling with experiment, require a full micromagnetic implementation coupled to the MEMS code.

The simple cantilever modeled here could be replaced by a membrane, this only requiring the geometrical properties of the model to be adjusted. The wireless nature of stimulation and interrogation of such sensors offers deployment of a passive sensor in hostile environments.

We are going on to consider the damping effects of working in fluids, with initial results, to be published later, indicating an acceptable response even in a viscous fluid.

These challenges can be met with the resources available, and the potential for application in security, healthcare and bio-science is obvious.

VI. Conclusion

A full integration of magnetomechanical and magnetoelastic models has produced a powerful package for the design of MEMS incorporating magnetic materials. The FEM has been validated with analytical solutions wherever possible. From the wide range of possible magnetic materials for such applications, it has been argued that high susceptibility and saturation magnetostriction constant, and low anisotropy field offer the best option.

Acknowledgment

References

[1] O. Cugat, J. Delamare, and G. Reyne, "Magnetic micro-actuators and systems (MAGMAS)," *IEEE Trans Magn.*, vol. 39, no. 6, pp. 3607–3612, Nov. 2003.

[2] J. W. Judy, "Microelectromechanical systems (MEMS): Fabrication design and applications," *Smart Mater. Struct.*, vol. 10, pp. 1115–1134, 2001.

[3] M. R. J. Gibbs, E. W. Hill, and P. J. Wright, "Magnetic materials for MEMS applications," *J. Phys. D.: Appl. Phys.*, vol. 37, pp. R237–R244, 2004.

[4] I. J. Busch-Vishniac, "The case for magnetically-driven micro-actuators," *Sens. Actuators A: Phys.*, vol. 33, pp. 207–220, 1992.

[5] I. Bolshakova, "Magnetic microsensors: Technology, properties, applications," *Sens. Actuators A: Phys.*, vol. 68, pp. 282–285, 1998.

[6] P. I. Nikitin, M. V. Valeiko, A. Y. Toporov, A. M. Ghorbanzadeh, and A. A. Beloglazov, "Deposition of thin ferromagnetic films for application in magnetic sensor microsystems," *Sens. Actuators A: Phys.*, vol. 68, pp. 442–446, 1998.

[7] H. Chiriac, M. Pletea, and E. Hristoforou, "Magnetoelastic characterization of thin films dedicated to magnetomechanical microsensor applications," *Sens. Actuators A: Phys.*, vol. 68, pp. 414–418, 1998.

[8] H. Chiriac, M. Pletea, and E. Hristoforou, "Fe-based amorphous thin film as a magnetoelastic sensor material," *Sens. Actuators A: Phys.*, vol. 81, pp. 166–169, 2000.

[9] R. Watts, M. R. J. Gibbs, W. J. Karl, and H. Szymczak, "Finite-element modelling of magnetostrictive bending of a coated cantilever," *Appl. Phys. Lett.*, vol. 70, pp. 2607–2609, 1997.

[10] J. Dean, M. R. J. Gibbs, and T. Schrefl, "Finite-element analysis on cantilever beams coated with magnetostrictive material," *IEEE Trans. Magn.*, vol. 42, no. 2, pp. 283–288, Feb. 2006.

[11] C. Body, G. Reyne, and G. Meunier, "Modeling of magnetostrictive thin films, application to a micromembrane," *J. Phys. III France*, vol. 7, pp. 67–85, 1997.

[12] J. D. Livingston, "Magnetomechanical properties of amorphous metals," *Phys. Stat. Sol. A.*, vol. 70, pp. 591–596, 1997.

[13] M. R. J. Gibbs, C. Shearwood, J. L. Dancaster, P. E. M. Frere, and A. J. Jacobs-Cook, "Piezomagnetic tuning of a micromachined resonator," *IEEE Trans. Magn.*, vol. 32, no. 5, pp. 4950–4952, Sep. 1996.

[14] P. T. Squire and M. R. J. Gibbs, "ΔE effect in obliquely field-annealed METGLAS® 2605SC," *IEEE Trans. Magn.*, vol. 25, no. 5, pp. 3614–3616, Sep. 1989.

[15] C. A. Grimes, P. G. Stoyanov, D. Kouzoudis, and K. G. Ong, "Remote query pressure measurement using magnetoelastic sensors," *Rev. Sci. Instrum.*, vol. 70, pp. 4711–4714, 1999.

[16] A. P. Thomas and M. R. J. Gibbs, "Anisotropy and magnetostriction in metallic glasses," *J. Magn. Magn. Mater.*, vol. 103, pp. 97–110, 1992.

[17] C. Shearwood, A. D. Mattingley, and M. R. J. Gibbs, "Growth and patterning of amorphous FeSiBC films," *J. Magn. Magn. Mater.*, vol. 162, pp. 147–154, 1996.

[18] M. Ali, R. Watts, W. J. Karl, and M. R. J. Gibbs, "The use of stress for the control of magnetic anisotropy in amorphous FeSiBC thin films: A magneto-optic study," *J. Magn. Magn. Mater.*, vol. 190, pp. 199–204, 1998.

[19] [Online]. Available: www.metglas.com. Accessed Oct. 17, 2006

[20] R. C. Hall, "Magnetic anisotropy and magnetostriction of ordered and disordered cobalt-iron alloys," *J. Appl. Phys.*, vol. 31, pp. 157S–158S, 1960.

[21] [Online]. Available: www.vacuumschmelze.de Accessed Oct. 17, 2006

[22] M. D. Cooke, M. R. J. Gibbs, and R. F. Pettifer, "Sputter deposition of compositional gradient magnetostrictive FeCo based thin films," *J. Magn. Magn. Mater.*, vol. 237, pp. 175–180, 2001.

[23] A. E. Clarke, J. B. Restorff, M. Wun-Fogle, T. A. Lograsso, and D. L. Schlagel, "Magnetostrictive properties of body-centered cubic Fe-Ga and Fe-Ga-Al alloys," *IEEE Trans. Magn.*, vol. 36, no. 5, pp. 3238–3240, Sep. 2000.

[24] A. Butera, J. Gomez, J. L. Weston, and J. A. Barnard, "Growth and magnetic characterization of epitaxial $Fe_{18}Ga_{19}$/MgO (100) thin films," *J. Appl. Phys.*, vol. 98, p. 033901, 2005.

[25] T. Honda, K. I. Aria, and M. Yamaguchi, "Fabrication of magnetostriction actuators using rare-earth (Tb,Sm)-Fe thin films (invited)," *J. Appl. Phys.*, vol. 76, pp. 6994–6999, 1994.

[26] T. Honda, K. I. Aria, and M. Yamaguchi, "Basic properties of magnetostictive actuators using Tb-Fe and Sm-Fe thin films," *IEICE Trans. Electron.*, vol. 80, pp. 232–238, 1997.

[27] V. H. Guerrero and R. C. Wetherhold, "Strain and stress calculation in bulk magnetostrictive materials and thin films," *J. Magn. Magn. Mater.*, vol. 271, pp. 190–206, 2004.

[28] B. Ilic, H. G. Craighead, S. Krlov, W. Senaratne, C. Ober, and P. Neuzil, "Attogram detection using nanoelectromechanical oscillators," *J. Appl. Phys.*, vol. 95, pp. 3694–3703, 2004.

[29] S. L. McArthur, private communication.